Neoplasma 2025; 72(6): 430–440

doi:10.4149/neo_2025_250720N317

PAF15 drives melanoma progression by promoting proliferation concomitant with suppression of DNA damage and apoptosis: a novel therapeutic vulnerability

Yacong JI[1,#], Chongyang LI[2,#], Han HAO[3], Yang LIU[4], Yan MAO[1], Leiyang GUO[1], Lichao LIU[1], Yaling LIU[1], Shaomin SHI[1,*]

[1]Department of Dermatology, Hebei Medical University Third Hospital, Shijiazhuang, Hebei, China; [2]Department of Medical Oncology, Shanghai Pulmonary Hospital, School of Medicine, Tongji University, Shanghai, China; [3]Center of Innovative Drug Research and Evaluation, Hebei Medical University, Shijiazhuang, Hebei, China; [4]Department of Pathology, Hebei General Hospital, Shijiazhuang, Hebei, China

**Correspondence: dermatologist_shi@163.com*
#Contributed equally to this work.

Received July 20, 2025 / Accepted December 8, 2025

PAF15 is an oncogene and is overexpressed across multiple malignancies. However, its biological role in melanoma remains largely unclear. In this research, bioinformatics analysis (GEPIA2, TCGA, CancerSEA) confirmed transcriptional PAF15 overexpression in melanoma, correlating with a poor prognosis and implicating pathways involved in cell cycle, proliferation, DNA damage, and repair. Immunohistochemical analysis further confirmed high expression of PAF15 protein in clinical melanoma tissues. Subsequently, the impact of PAF15 on melanoma cell proliferation and cell cycle progression was quantified through MTT assay and propidium iodide staining. Annexin V staining and immunofluorescence were used to assess apoptosis and DNA damage. Markers associated with these biological pathways were evaluated by western blot. Evaluation of PAF15-mediated tumorigenic effects was performed using a subcutaneous xenograft model. The results revealed that PAF15 knockdown markedly suppressed melanoma cell proliferation through the induction of G0/G1 phase cell cycle arrest. Additionally, PAF15 knockdown triggered genomic instability, as evidenced by increased DNA damage markers, and promoted caspase-dependent apoptosis. Furthermore, PAF15 knockdown suppressed the growth of xenograft tumors in vivo. Notably, these tumor-inhibiting effects of PAF15 knockdown were effectively rescued upon PAF15 reconstitution. Summed up, these findings establish PAF15 as both a prognostic indicator for unfavorable clinical outcomes and a promising therapeutic vulnerability in melanoma.

Key words: melanoma; PAF15; proliferation; DNA damage; apoptosis

Melanoma is the most lethal type of skin cancer that originates from the malignant transformation of melanocytes [1]. The incidence rate of melanoma continues to increase steadily [2]. With the deepening of research on the pathogenesis and molecular basis of melanoma, a growing number of oncogenic genes have been identified as therapeutic targets [3, 4]. For example, the application of BRAF inhibitors and MEK inhibitors significantly improved the survival of melanoma patients. Unfortunately, many patients still do not respond to these treatments or develop resistance [3, 4]. Therefore, the identification and functional characterization of novel genetic markers with dual prognostic and therapeutic potential represents a critical unmet need in precision oncology.

Proliferating cell nuclear antigen (PCNA) – associated factor (PCLAF/PAF15, hereafter written as PAF15), also referred to as KIAA0101/NS5ATP9/OEACT-1, was initially identified as a PCNA binding partner [5]. It interacts with the PCNA ring via a conserved PCNA-interacting protein motif, which engages with the sliding surface of PCNA [6]. While the direct DNA-PCNA interaction is extremely weak and unspecific to be detected, PAF15 binds DNA through its histone-like N-terminal tail and therefore regulates PCNA sliding along the DNA [6]. Considering that PCNA can recruit various factors involved in DNA repair and cell cycle regulation to the replication fork [7], it is plausible that PAF15 may be implicated in DNA replication, DNA repair, and cell cycle regulation. Notably, PAF15 can also function

independently of PCNA. For instance, PAF15 has been shown to co-immunoprecipitate with p33ING1b, indicating a potential interaction between PAF15 and p33ING1b [8]. In pancreatic cancer, PAF15 drives tumorigenesis by hyperactivating MAPK signaling through transcriptional activation of LAMTOR3, a scaffolding protein that enhances MEK and ERK phosphorylation dynamics [9]. It can also restrain the interaction between p53 and Sp1 in breast cancer, thus promoting cell proliferation [10]. A pan-cancer study showed that PAF15 was barely expressed in normal cells but frequently overexpressed in various cancer cells, and significantly correlated with poor prognosis [11]. Overall, PAF15 is associated with poor prognosis in multiple cancers and regulates cellular processes such as proliferation and apoptosis. However, its biological function in melanoma remains largely unclear.

This study systematically investigated the biological functions of PAF15 in melanoma pathogenesis. Clinical data analysis revealed that PAF15 is significantly overexpressed in melanoma tissues and strongly correlates with poor patient prognosis. Mechanistic studies demonstrated that PAF15 knockdown markedly inhibits cell proliferation, induces G0/G1 phase arrest, and promotes DNA damage and apoptosis. Furthermore, *in vivo* experiments confirmed that PAF15 knockdown effectively suppresses tumorigenicity. These findings collectively establish PAF15 as a clinically relevant prognostic biomarker and a potential therapeutic target.

Materials and methods

Bioinformatics analyses. The expression levels of PAF15 (KIAA0101) mRNA in melanoma and normal tissues were generated by the GEPIA2 online tool (http://gepia2.cancer-pku.cn/#index) [12]. For survival analysis, the prognostic role of PAF15 on disease-specific survival (DSS) and progression-free interval (PFI) of melanoma patients was explored. The expression data of PAF15 were derived from RNA-seq data of TCGA, and the "EBPlusPlusAdjustPANCAN_illumina-HiSeq_SNASeqV2.geneExp.tsv" file was downloaded from PanCanAtlas (https://gdc.cancer.gov/about-data/publications/pancanatlas) [13]. Then the expression level of PAF15 in melanoma was extracted and standardized to a z-score [14]. Kaplan-Meier survival analysis was subsequently performed using the R package "survival"; the optimal cut-off values of the high/low expression cohort were determined by the R package "survminer" (the minimum proportion of the high/low expression group should not be less than 0.2). The significance between the high and low expression groups was evaluated by the log-rank test using the survfit function. For functional analysis of PAF15, the package "TCGAplot" was used for PAF15 coexpression analysis and Gene Ontology (GO) enrichment [15]. Gene Set Enrichment Analysis (GSEA) by MAGeCKFlute of TCGA data was performed between PAF15-high and PAF15-low samples (the highest 50% versus the lowest 50%), and results were shown by the GSEAVis package (https://github.com/junjunlab/GseaVis) [16, 17]. The CancerSEA database (http://biocc.hrbmu.edu.cn/CancerSEA) was employed, which has compiled 14 different functional states of tumor cells [18]. The Z-score is an algorithm proposed by Lee et al. [14] that integrates the expression of signature genes to reflect the activity of a given pathway. We used the z-score parameter in the R package GSVA to calculate the combined z-score of 14 functional state gene sets [19]. Pearson correlation analysis was performed to calculate the statistical correlation between the genes and each z-score.

Cell lines and cell culture. Human melanoma cell lines A375, SKMEL28, and human embryonic kidney (HEK) 293T cell line were obtained from the American Type Culture Collection (ATCC, USA). All cells were fostered in a 37 °C incubator containing 5% CO_2. A375, SKMEL28, and HEK293T cells were cultured in Dulbecco's Modified Eagle's Medium (DMEM, Gibco, USA) supplemented with 10% fetal bovine serum (FBS, Gibco) and 1% penicillin-streptomycin solution (Biological Industries, Israel). All cell lines used in this study were confirmed to be free of mycoplasma contamination using the Luminescent Mycoplasma Detection Kit (Beyotime, China).

Transfection and infection. For PAF15 knockdown, lentiviral vectors containing PAF15 shRNA plasmids were procured from YouBio (China). The shRNA sequences used were as follows: shPAF15-1#: 5'-GCAACCTGATCACACAAATGA-3'; shPAF15-2#: 5'-GCTTTGTTGAACAGGCATTTA-3'; shGFP: 5'-CAAGCTGACCCTGAAGTTCAT-3'. For PAF15 re-expression, a PAF15-overexpression plasmid (pCDH-CMV-MCS-EF1-GFP-Puro-PAF15) was purchased from YouBio, and an empty vector was used as a control. Target plasmids, packaging plasmids (pLP1, pLP2, pLP/VSVG), and Lipofectamine were co-transferred into HEK293T cells. The virus was collected 48 h post-transfection. Melanoma cell lines A375 and SKMEL28 were then infected with the virus to generate stable transfected cells. PAF15 knockdown cells (shPAF15-2# targeting the 3'UTR sites) were infected with a PAF15 overexpression virus for PAF15 re-expression and rescue tests.

3-(4,5-dimethylthiazol-2-yl)-2,5-diphenyltetrazolium bromide (MTT) assay. A 96-well plate was seeded with 5×10^3 cells per well. After 24 h and 48 h of culturing, the MTT assay was performed to assess cell viability. Briefly, 20 μl MTT (5 mg/ml) solution was added to each well and incubated for 4 h. After that, the medium was removed, and 200 μl of DMSO was added to each well to dissolve the generated formazan. The absorbance at 560 nm was measured by a microplate reader (Thermo Fisher, USA).

Flow cytometric analysis. Cells were collected after 48 h of culturing and washed twice with PBS. For cell cycle analysis, cells were fixed in 75% ethanol at 4 °C overnight. After PBS washing, the cells were then resuspended in PBS containing 50 μg/ml propidium iodide (PI, Beyotime) and 10 μg/ml RNase A (Beyotime), followed by 30 min of

incubation at room temperature in the dark. For apoptosis assessment, Annexin V-FITC&PI Apoptosis Detection Kit (Sangon Biotech, China) was utilized. Detailed operations were in accordance with the manufacturer's protocol. Finally, the cells were analyzed via a flow cytometer (BD, USA) and FlowJo software.

Immunofluorescence staining. An immunofluorescence assay was performed to detect the expression of γ-H2AX in melanoma cells. Briefly, the cells were collected after 48 h of culturing and fixed with 4% paraformaldehyde for 20 min at room temperature, followed by 30 min of permeabilization with 0.3% Triton X-100. Thereafter, blocked with 5% goat serum (Sigma, USA) for 2 h at room temperature and incubated with γ-H2AX antibody (1:400, #9718, CST, USA) at 4 °C overnight. Subsequently, the samples were incubated with Alexa Fluor 594-labeled secondary antibody (1:1000, #A-11005, Thermo Fisher) for 2 h in the dark. Finally, the nuclei were stained with DAPI for 20 min. The Olympus FV1000 confocal fluorescence microscope was used for observation and image acquisition.

Western blots. Cells were lysed in RIPA buffer (Beyotime) containing protease/phosphatase inhibitor cocktail (Beyotime). Protein concentration was measured using the BCA Protein Assay Kit (Beyotime). Equivalent amounts of each sample were loaded on 8–12% Bis-Tris gels (Beyotime), transferred to polyvinylidene difluoride (PVDF) membranes, and immunoblotted with following primary antibodies at the suggested dilutions: PAF15 (#sc-390515, Santa Cruz, USA), CDK4 (#66950-1-Ig, Proteintech, China), CDK6 (#14052-1-AP, Proteintech), Cyclin D1 (#60186-1-Ig, Proteintech), Cleaved Caspase-3 (#9664, CST), Cleaved PARP (#5625, CST), γ-H2AX (#9718, CST), phospho-ATM (p-ATM, #5883, CST), α-Tubulin (#AF5012, Beyotime) for overnight at 4 °C. On the following day, the sections were washed three times with TBST, then incubated with secondary antibodies HRP-labeled goat anti-rabbit IgG (#A0208, Beyotime) or goat anti-mouse IgG (#A0216, Beyotime) at room temperature for 2 h. After the incubation, the sections were washed three times with TBST. Finally, images were captured using the Chemiscope imaging system (Clinx, China) with BeyoECL Plus reagent (Beyotime).

Tumor xenograft assay. Animal experiments were approved and supervised by the Institutional Animal Care and Use Committee of Hebei Medical University (Approval number: IACUC-Hebmu-P 2024135). Four-week-old female BALB/c nude mice were purchased from HFK Bioscience Co., Ltd. (China). Specific pathogen-free facilities were used for housing and care of all mice. After 7 days of environmental adaptation, 18 mice were randomly distributed into three groups (6 in each group). Next, three types of A375 cells (shGFP, shPAF15, and shPAF15+PAF15) were subcutaneously injected into the right flank region of the mice according to the predetermined grouping, 1×10^6 cells per mouse. Since the 10th day, tumor length (L) and width (W) were measured every 4 days, and the volume was calculated using the formula: Volume = $L \times W^2 \times \pi/6$. Thirty days after injection, the mice were euthanized, tumor from each mouse was weighed and stored for further analysis.

Immunohistochemical (IHC) staining. For the IHC staining assay of clinical melanoma (n=16) and benign nevi (n=20) tissues, samples were collected from Hebei Medical University Third Hospital. The use of patient material was approved and supervised by the Ethics Committee of Hebei Medical University Third Hospital (Approval number: 2024-041-1). For the IHC staining assay of mouse xenografts, the tumors were collected for subsequent experiments. The tissues were fixed in 4% paraformaldehyde for 72 h, and then dehydrated in an automatic dehydrator. After being embedded in paraffin, 4 μm-thick slices were made. Then, dewaxed through gradient xylene and alcohol, followed by antigen retrieval with 10 mM citrate buffer (pH 6.0) under microwave heating for 10 min. Subsequently, the sections were incubated in 1% Triton for 1 h, then treated with endogenous peroxidase inhibitor at room temperature for 10 min. Following washing with PBS, the sections were blocked with 5% goat serum at room temperature for 1 h and incubated overnight in the dark with PAF15 (1:200, #sc-390515, Santa Cruz) and Ki-67 (1:4000, #27309-1-AP, Proteintech) antibodies at 4 °C. Following this, HRP-labeled secondary antibodies were added for 20 min of further immune reaction at room temperature, and DAB was used for staining. Next, the slices were counterstained using hematoxylin and dehydrated through gradient alcohol and xylene. Finally, the sections were sealed with neutral resin and coverslips. Cell staining positivity rate was calculated after observation and photography under an optical microscope.

Statistical analysis. Statistical analyses were conducted using GraphPad Prism 6.0. Data were expressed as mean ± SD or mean ± SEM of at least three independent repetitions. Comparisons between two groups were conducted using the unpaired two-tailed Student's t-test. One-way ANOVA followed by Tukey's test was done to determine the significance of differences among multiple groups. The value of $p<0.05$ was considered statistically significant. Significance was denoted as: *$p<0.05$, **$p<0.01$, and ***$p<0.001$.

Results

Overexpression of PAF15 in melanoma is correlated with adverse clinical outcomes. We first used a publicly available dataset, GEPIA2, to assess the expression level of PAF15 in melanoma. PAF15 is overexpressed in melanoma compared to normal tissues (Figure 1A), consistent with its expression profile in multiple cancer types. Furthermore, comprehensive survival analysis of the TCGA skin cutaneous melanoma (SKCM) cohort revealed that elevated PAF15 expression levels were significantly associated with reduced DSS and shorter PFI, underscoring its prognostic relevance in melanoma progression (Figures 1B, 1C). To validate the

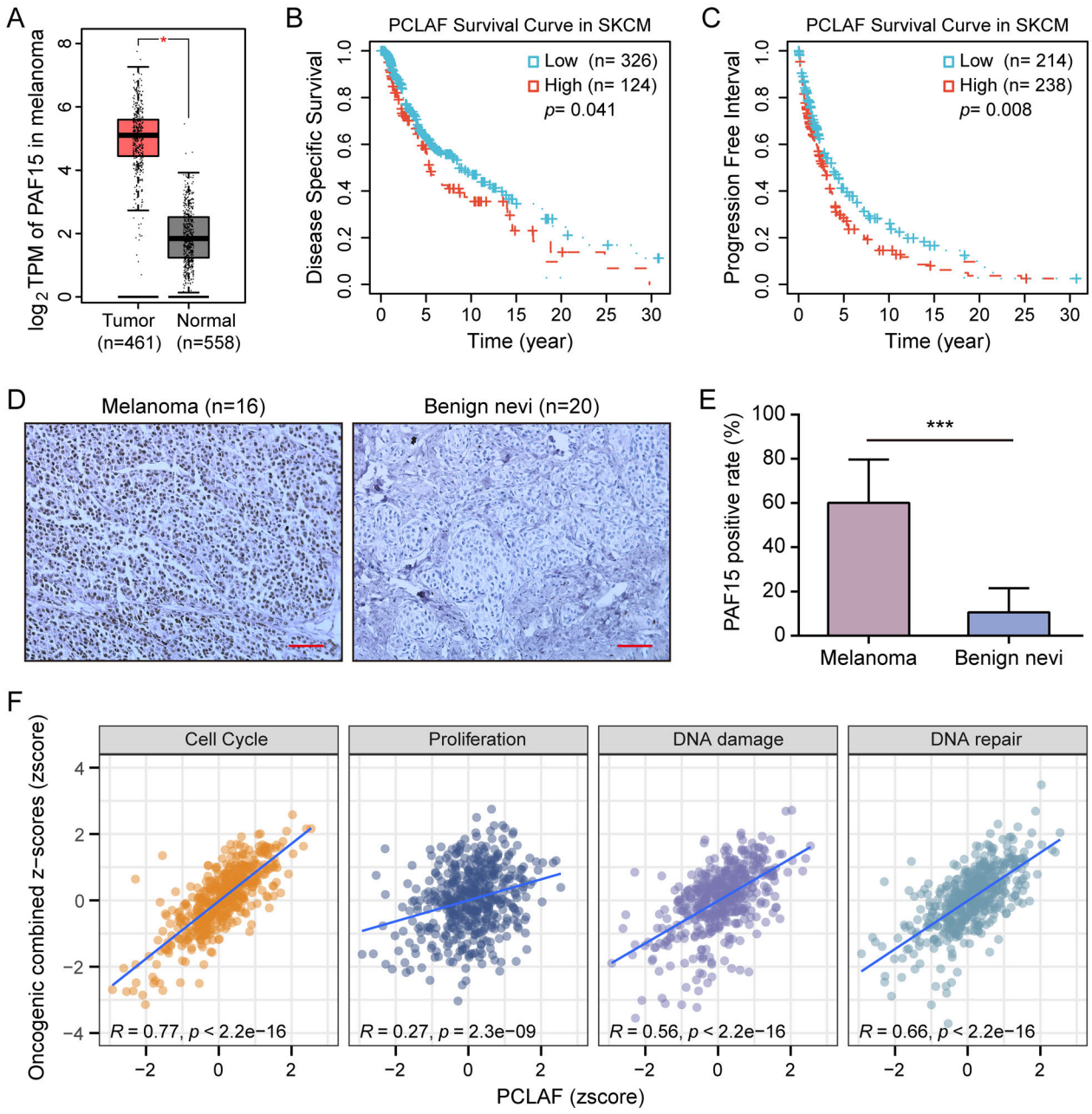

Figure 1. Expression level and roles of PAF15 in melanoma. A) The mRNA expression of PAF15 in melanoma and normal tissues. B, C) Disease-specific survival and progression-free interval of PAF15-high and PAF15-low patients in TCGA. D, E) Representative images of IHC staining of PAF15 in human melanoma and benign nevi tissues. Scale bar, 200 μm. PAF15 positive rate was calculated (mean ± SD, unpaired two-tailed Student's t-test). F) Signature scores of cell cycle (R=0.77), cell proliferation (R=0.27), DNA damage (*R*=0.56), and DNA repair (R=0.66) pathways at single cell solution of melanoma defined by CancerSEA database. *p<0.05, ***p<0.001

upregulation of PAF15 protein in melanoma, we collected clinical samples from patients with melanoma and benign nevi. IHC analysis revealed a significantly higher expression level of PAF15 protein in melanoma tissues compared to benign nevi (Figures 1D, 1E). We then explored the functions of PAF15 using the CancerSEA database. PAF15 was found to be mainly related to cell cycle, cell proliferation, DNA damage, and DNA repair (Figure 1F). GO enrichment analysis of PAF15 co-expressed genes in the TCGA-SKCM transcriptomic data revealed significant enrichment of cell cycle-related biological processes, like chromosome segregation (Supplementary Figures S1A, S1B). Consistent with

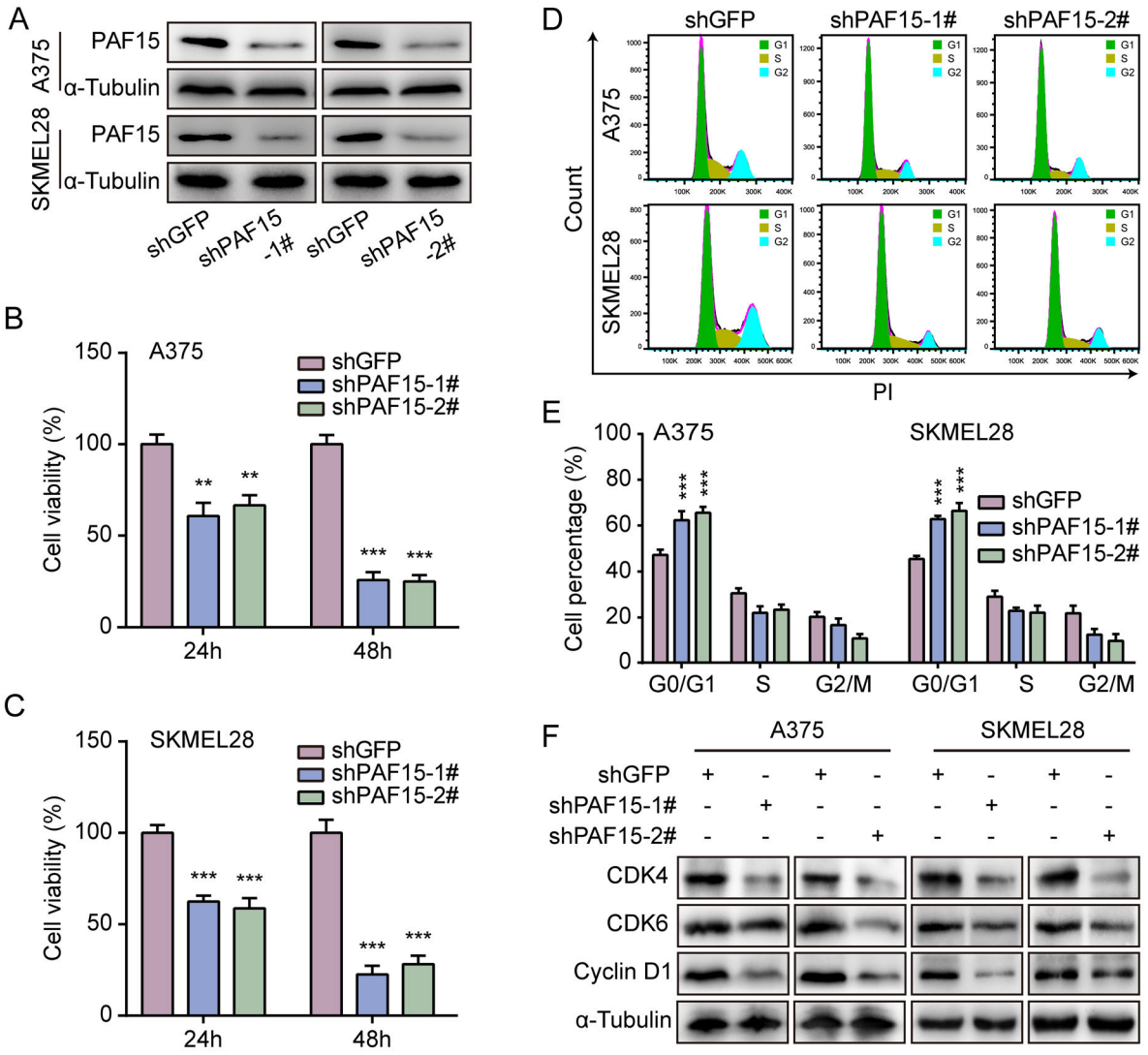

Figure 2. PAF15 knockdown inhibits melanoma cell proliferation and induces cell cycle arrest. A) Western blot analyses show the knocking down of PAF15 in A375 and SKMEL28 cells. B, C) After 24 h and 48 h of cultivation, the viability of A375 and SKMEL28 cells with PAF15 or GFP knockdown was measured by MTT assay (mean ± SD, one-way ANOVA followed by Tukey's test). D, E) Cell cycle assessment by flow cytometry analyses in A375 and SKMEL28 cells with PAF15 or GFP knockdown. The cell population in each phase of the cell cycle was quantified (mean ± SD, one-way ANOVA followed by Tukey's test). F) Western blot analyses of the CDK4, CDK6, and cyclin D1 expression levels in A375 and SKMEL28 cells with PAF15 or GFP knockdown. **p<0.01, ***p<0.001

these results, GSEA between PAF15-high and PAF15-low TCGA-SKCM samples showed that PAF15 was closely linked to DNA replication, cell cycle regulation, and proliferation (Supplementary Figures S1C, S1D). Collectively, these data revealed that PAF15 is overexpressed in melanoma and is involved in proliferation-related cellular processes, which correlates with adverse clinical outcomes.

PAF15 knockdown inhibits cell proliferation and induces G0/G1 cell cycle arrest in melanoma. To establish stable PAF15-knockdown melanoma models, shRNAs were transfected into 2 melanoma cell lines, A375 and SKMEL28. Knockdown efficiency was evaluated by immunoblotting (Figure 2A). To evaluate the impact of PAF15 knockdown on proliferative capacity, MTT assays were performed after 24 h and 48 h of culturing. PAF15 knockdown significantly reduced cell viability in a time-dependent manner (Figures 2B, 2C). Furthermore, cell cycle analysis by flow cytometry showed that knockdown of PAF15 in A375 and SKMEL28 cell lines resulted in an increased percentage of cells in the G0/G1 phase (Figures 2D, 2E). The activity of cyclin D1 and CDK4/6 plays a central role in the promotion of cell cycle entry [20]; therefore, we evaluated their expression by

immunoblotting. As expected, CDK4, CDK6, and cyclin D1 were downregulated in PAF15-knockdown melanoma cells (Figure 2F). These results showed that PAF15 knockdown significantly inhibited cell proliferation.

Attenuated PAF15 levels induce DNA repair deficiency and apoptosis in melanoma. Previous studies have shown that PAF15 deficiency impairs DNA repair and induces apoptosis in certain cellular contexts [21]. However, silencing of PAF15 does not affect apoptosis in some cancer models [22]. In our melanoma cell lines, knocking down PAF15 led to an increased proportion of apoptotic cells (Figures 3A, 3B). Immunofluorescence staining revealed that the levels of γ-H2AX, a DNA damage marker, also significantly increased (Figures 3C, 3D). Immunoblotting of apoptosis (Cleaved

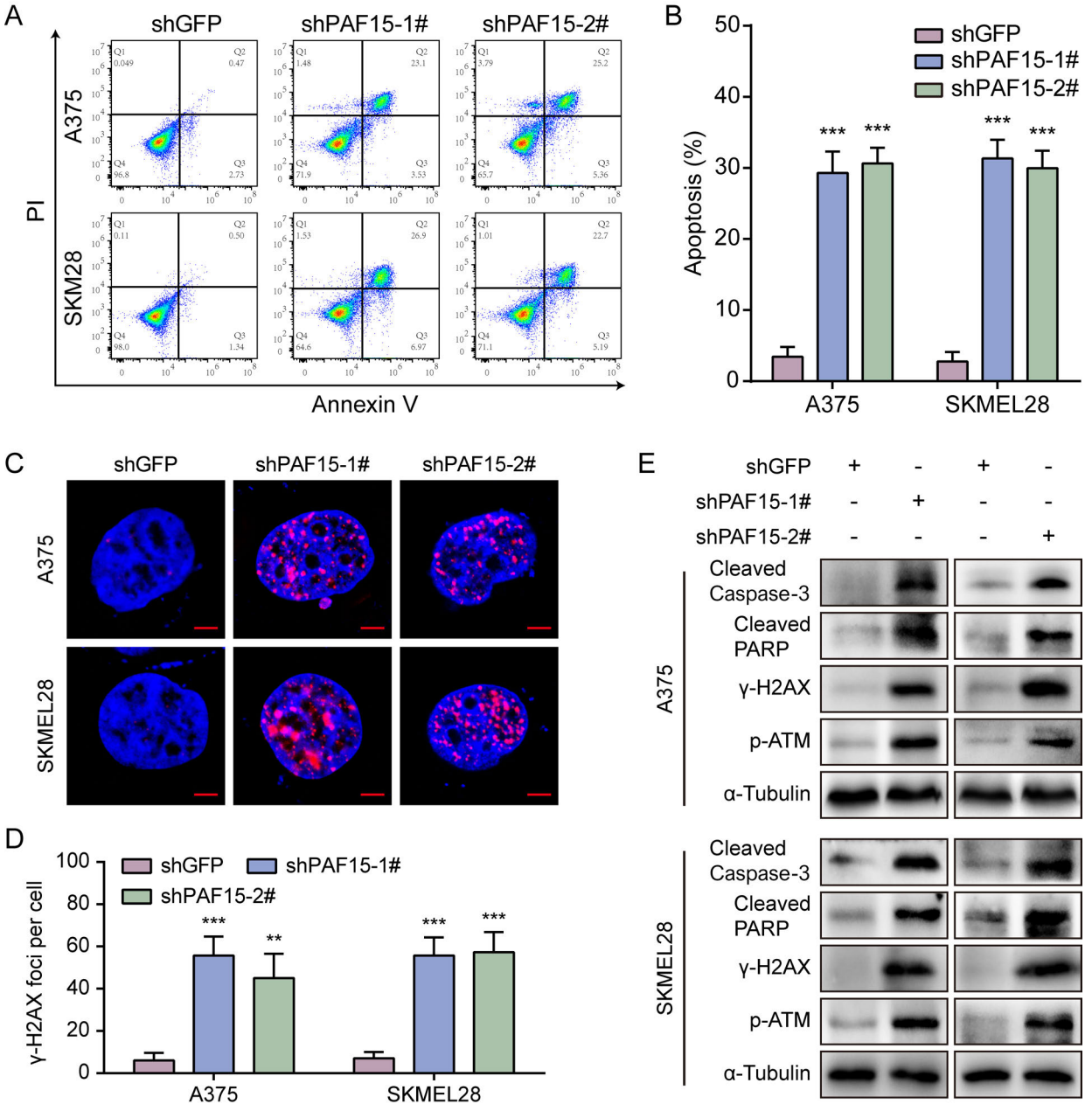

Figure 3. PAF15 knockdown induces DNA damage and apoptosis in melanoma cells. A, B) Apoptosis assessment by flow cytometry analyses in A375 and SKMEL28 cells with PAF15 or GFP knockdown. The apoptotic rate of the cells was quantified (mean ± SD, one-way ANOVA followed by Tukey's test). C, D) Immunofluorescence assay was used to show the γ-H2AX in A375 and SKMEL28 cells with PAF15 or GFP knockdown. Scale bar, 5 μm. The number of foci per cell was calculated (mean ± SD, one-way ANOVA followed by Tukey's test). E) Western blot analysis depicted the expression of apoptosis (Cleaved Caspase-3, Cleaved PARP) and DNA damage (γ-H2AX, P-ATM) markers in A375 and SKMEL28 cells with PAF15 or GFP knockdown. **p<0.01, ***p<0.001

Caspase-3, Cleaved PARP) and DNA damage (γ-H2AX, p-ATM) markers further confirmed the upregulation of DNA damage and apoptosis (Figure 3E). These data demonstrate that knockdown of PAF15 hinders cellular DNA repair and induces apoptosis.

PAF15 re-expression restores proliferation, DNA repair, and reduces apoptosis. To validate the specificity of our findings and exclude potential shRNA off-target effects, we performed rescue experiments by overexpressing PAF15 in knockdown cells (Figure 4A) and repeated the experiments. As data show, PAF15 re-expression successfully rescued cell viability (Figures 4B, 4C) and alleviated G0/G1 phase arrest (Figures 4D, 4E). To further substantiate this, we found that re-introducing PAF15 restored the expression levels of CDK4, CDK6, and cyclin D1, which had been altered by PAF15 knockdown (Figures 4F, 4G). Moreover, both apoptotic cell populations (Figures 5A, 5B) and DNA damage level (Figures 5C, 5D) were significantly decreased after PAF15 re-expression. Accordingly, the changes in Cleaved Caspase-3, Cleaved PARP, γ-H2AX, and p-ATM expression induced by PAF15 knockdown were restored (Figure 5E). These results conclusively demonstrate that PAF15 plays an essential role in regulating melanoma cell proliferation, genomic stability, and apoptosis.

PAF15 enhances melanoma tumor growth *in vivo*. To evaluate the role of PAF15 in melanoma progression *in vivo*, we established a subcutaneous xenograft model with A375 cells in BALB/c nude mice. Compared to the control group, PAF15-knockdown tumors exhibited significantly reduced tumor volume and weight, which were partially rescued by PAF15 re-expression (Figures 6A, 6B). IHC analysis of tumor tissues revealed that PAF15 knockdown significantly decreased Ki-67-positive cells, and this proliferative suppression was reversed upon PAF15 overexpression (Figures 6C, 6D). These data illustrated that PAF15 promotes tumor growth *in vivo*.

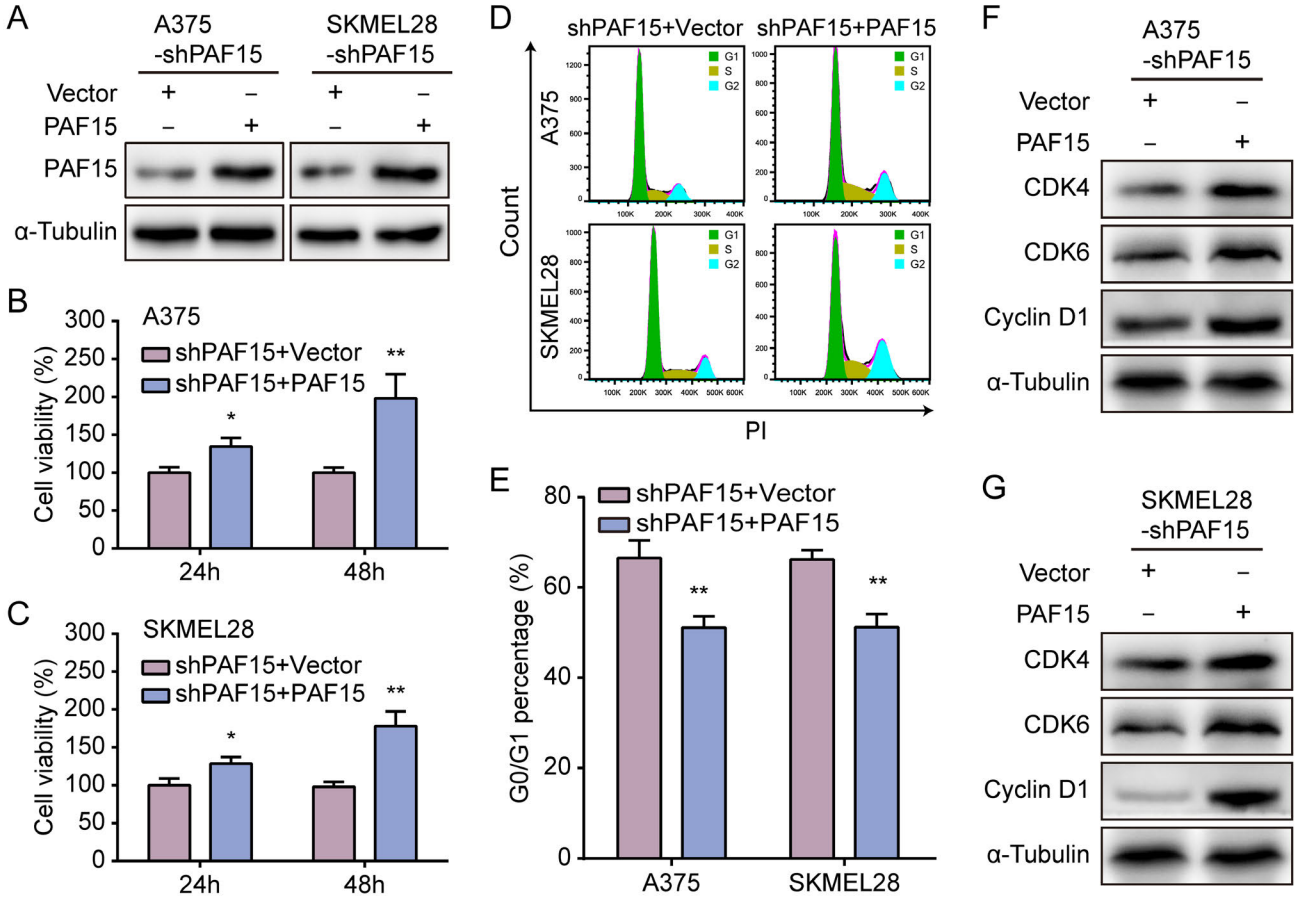

Figure 4. PAF15 overexpression restores cell viability and proliferation. A) Western blot analyses show the restoration of PAF15 expression in PAF15-knockdown A375 and SKMEL28 cells. B, C) Viability of PAF15 restoration A375 and SKMEL28 cells measured by MTT assay after 24 h and 48 h of culturing (mean ± SD, unpaired two-tailed Student's t-test). D, E) Cell cycle assessment by flow cytometry analyses in PAF15-knockdown A375 and SKMEL28 cells overexpressing PAF15 or not. The percentage of cells in G0/G1 phase is shown in a histogram (mean ± SD, unpaired two-tailed Student's t-test). F, G) Western blot analyses of the CDK4, CDK6, and cyclin D1 expression levels in PAF15-knockdown A375 and SKMEL28 cells overexpressing PAF15 or not. *p<0.05, **p<0.01

Discussion

Previous studies have found that PAF15 is highly expressed in a variety of tumors [11], such as lung cancer [22], neuroblastoma [23], pancreatic cancer [24], and breast cancer [25], which correlated with poor prognosis. However, conflicting evidence suggests that PAF15 is downregulated in hepatocellular carcinoma tissues, where its overexpression has been shown to suppress cancer cell proliferation [26]. These discrepancies may arise from individual differences or tumor heterogeneity, as indicated by contrasting findings in another study on hepatocellular carcinoma [27]. These observations suggest that the role of PAF15 may vary across different tumor types. In this study, by exploring public data, we discovered that PAF15 was highly expressed in melanoma, which significantly reduced the DSS and PFI of melanoma patients, suggesting that the high expression of PAF15 serves as a risk factor for melanoma progression. Additionally, the IHC study revealed that the expression of PAF15 protein in melanoma was significantly higher than in benign nevi. To the best of our knowledge, there are currently few reports on the expression level of PAF15 protein in human cutaneous melanoma tissues. Our study provides crucial evidence of its upregulation and highlights the potential diagnostic utility of PAF15 for the differential diagnosis between cutaneous melanoma and benign nevi.

In this study, knocking down PAF15 significantly inhibited melanoma cell proliferation. Further mechanistic studies revealed that this may be attributed to the effect of PAF15 knockdown on the cell cycle and cell cycle-related proteins, such as CDK4/6. Previous studies have shown that blocking PAF15-PCNA interaction can inhibit pancreatic cancer cell proliferation [24], suggesting that PAF15 promotes cell proliferation at least partially via PCNA. Mechanically, PAF15 hyperactivates a series of other signaling pathways, which promote tumor progression. Specifically, PAF15 inhibits the recruitment of p130 to the multi-vulval class B (MuvB) complex, which is essential for the transactivation of cell proliferation-related DREAM (dimerization partner, RB-like, E2F, and MuvB) complex target genes, thereby enabling cells to bypass cell cycle arrest [22]. Moreover, PAF15 regulates the expression of pituitary tumor-transforming gene 1 (PTTG1) via the transcription factor E2F1 and accelerates G1/S transition of neuroblastoma cell cycle [23]. These findings align with our observations that knockdown of PAF15 induces G0/G1 phase cell

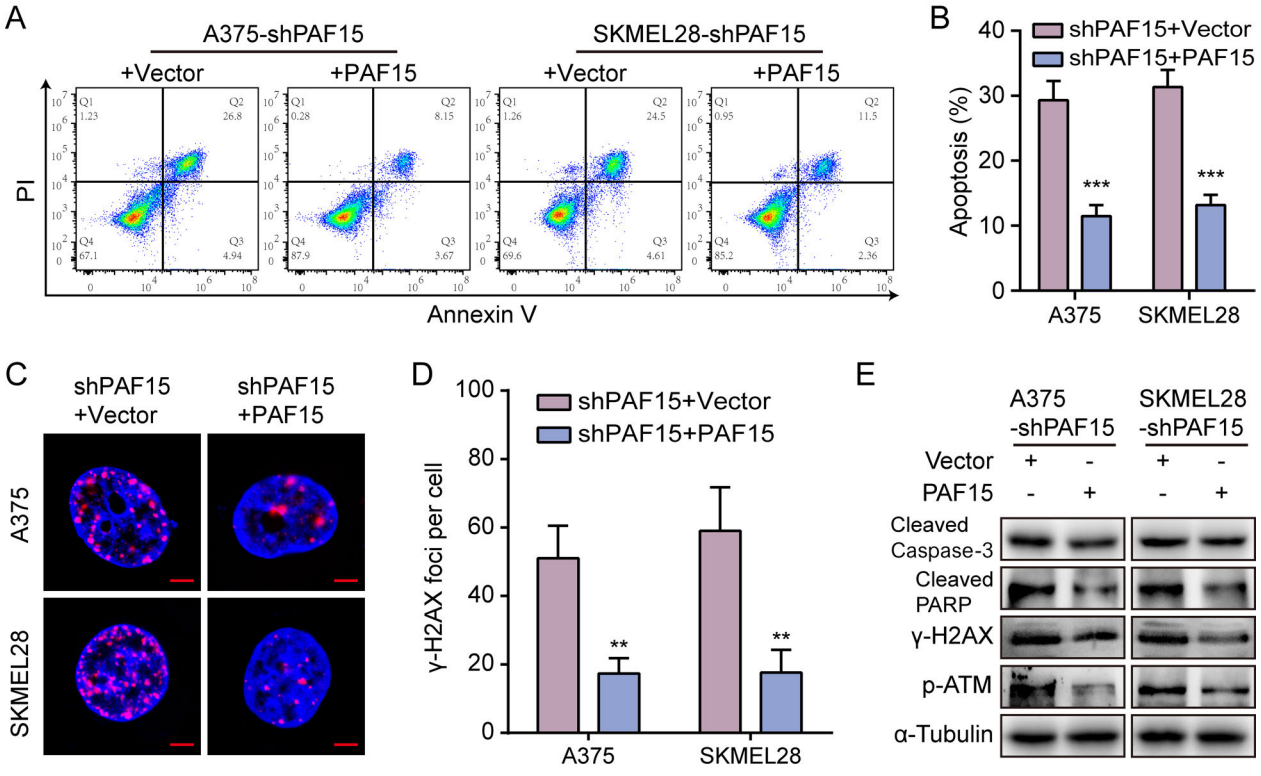

Figure 5. PAF15 overexpression restores DNA repair and apoptosis. A, B) Apoptosis assessment by flow cytometry analyses in PAF15-knockdown A375 and SKMEL28 cells overexpressing PAF15 or not. The apoptotic rate of the cells was quantified (mean ± SD, unpaired two-tailed Student's t-test). C, D) Immunofluorescence assay was used to show the γ-H2AX in PAF15-knockdown A375 and SKMEL28 cells overexpressing PAF15 or not. Scale bar, 5 μm. The number of foci per cell was calculated (mean ± SD, unpaired two-tailed Student's t-test). E) Western blot analyses depicted the expression of apoptosis (Cleaved Caspase-3, Cleaved PARP) and DNA damage (γ-H2AX, P-ATM) markers in PAF15-knockdown A375 and SKMEL28 cells overexpressing PAF15 or not. **p<0.01, ***p<0.001

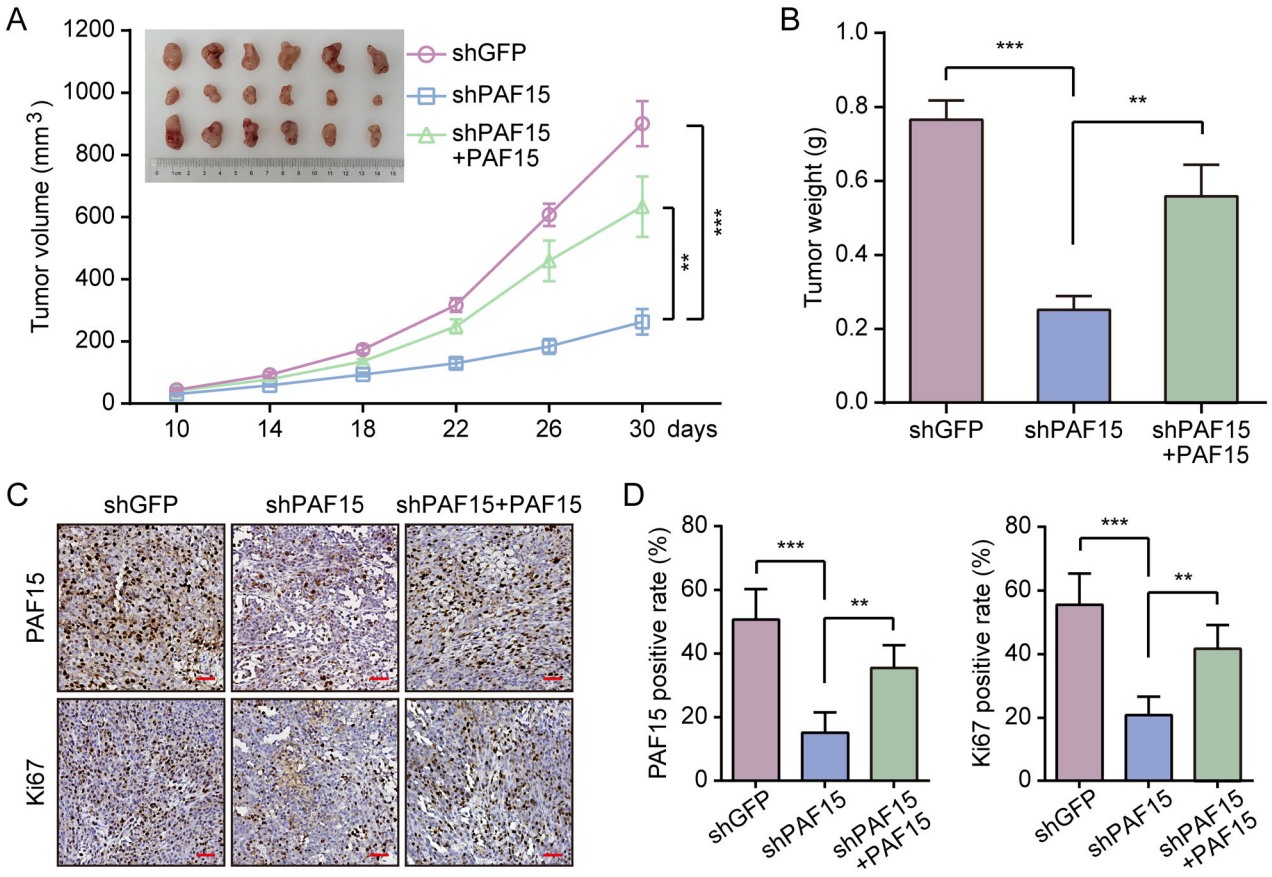

Figure 6. PAF15 promotes melanoma growth *in vivo*. A, B) The diagram demonstrates the subcutaneous xenograft tumors in mice formed by PAF15-knockdown A375 cells overexpressing PAF15 or not. The GFP-knockdown was used as a control group. The volumes and weights of the xenografts were measured (mean ± SEM, one-way ANOVA followed by Tukey's test). C) Representative IHC staining images of PAF15 and Ki-67 of the subcutaneous tumors. Scale bar, 100 μm. D) PAF15 and Ki-67-positive rate in the xenografts were calculated (mean ± SD, One-way ANOVA followed by Tukey's test). **p<0.01 and ***p<0.001

cycle arrest in melanoma cells. Interestingly, a recent single-cell analysis study on acral melanoma (AM) found that a distinct PAF15+ melanoma cell subpopulation drives tumor progression [28]. This subpopulation exhibits high stemness, enhanced proliferation, and activated E2F transcription factors and glycolytic metabolism. Its specific interactions via the AGRN and TGF-β signaling pathways further underscore the critical role of PAF15 in AM malignancy.

Our study revealed that PAF15 promoted melanoma progression, partially by inhibiting apoptosis; however, the detailed signaling pathway involved was not well understood. Recent mechanistic studies have provided insights into the molecular pathways underlying PAF15's functional roles in cellular processes and cancer pathogenesis. For instance, PAF15 can inhibit the transcription of p53 [29], an important gene that mediates apoptosis in cells with DNA double-strand breaks [30], thus decreasing the expression of p53-targeting genes and preventing liver cancer cell apoptosis. In colorectal cancer, inhibition of PAF15 induces apoptosis, marked by increased caspase 3/7 activity and suppression of the anti-apoptotic protein Bcl-2 [31]. Similarly, another study demonstrated that PAF15 upregulates Bcl-2 and downregulates key pro-apoptotic proteins, including cleaved caspase-9, cleaved caspase-7, cleaved PARP, and Bax, in ovarian cancer [32]. It was established that silencing PAF15 inhibited glycolysis, suppressed cell proliferation, and induced apoptosis in ovarian cancer. These effects were effectively rescued by the pharmacological reactivation of YAP, confirming YAP as a key downstream effector of PAF15 [33]. Overall, in different cancers, PAF15 may promote cell proliferation and inhibit apoptosis through different mechanisms.

Several studies have explored cancer treatment strategies by inhibiting PAF15. Recently, drugs that promote PAF15 degradation have been developed by proteolysis- targeting chimera (PROTACs) [34]. These compounds demonstrated potent antitumor activity *in vitro*, characterized by G0/G1 cell cycle arrest and induction of apoptosis. The attenuation of PAF15 has been shown to downregulate c-Myc, an important oncogene, and weaken the stemness of colorectal cancer cells, which is required for intestinal tumorigenesis

[35]. Moreover, elevated PAF15 expression reduced chemotherapy sensitivity of esophageal cancer cells *in vitro* [36] and is a marker of recurrence in gastric cancer after surgery [37]. Knockdown of PAF15 increased radiosensitivity in non-small cell lung cancer [38], partially through the Wnt/β-catenin signaling pathway. Therefore, targeting PAF15 may serve as a strategy to increase the efficiency of chemotherapy or radiotherapy. These studies, consistent with our results, which show that PAF15 knockdown inhibits melanoma cell proliferation and induces DNA damage and apoptosis, further confirm the druggable value of PAF15 in melanoma.

In conclusion, our study demonstrates that PAF15 knockdown suppresses melanoma progression through multiple mechanisms, including induction of G0/G1 cell cycle arrest, promotion of DNA damage, and activation of apoptotic pathways. These findings suggest that PAF15 plays a critical role in melanoma pathogenesis and may serve as both a prognostic marker and a potential therapeutic target for melanoma treatment.

Supplementary information is available in the online version of the paper.

Acknowledgments: This study was funded by grants from Hebei Natural Science Foundation (Grant number: H2022206446); Medical Science Research Project of Hebei Province (Grant number: 20250005); The Postdoctoral Fellowship Program of CPSF (Grant number: GZB20240544); The China Postdoctoral Science Foundation (Grant number: 2024M752432); The Natural Science Foundation of Shanghai (Grant number: 24ZR1469100).

References

[1] SHAIN AH, BASTIAN BC. From melanocytes to melanomas. Nat Rev Cancer 2016; 16: 345–358. https://doi.org/10.1038/nrc.2016.37

[2] LONG GV, SWETTER SM, MENZIES AM, GERSHENWALD JE, SCOLYER RA. Cutaneous melanoma. Lancet 2023; 402: 485–502. https://doi.org/10.1016/S0140-6736(23)00821-8

[3] LUKE JJ, FLAHERTY KT, RIBAS A, LONG GV. Targeted agents and immunotherapies: optimizing outcomes in melanoma. Nat Rev Clin Oncol 2017; 14: 463–482. https://doi.org/10.1038/nrclinonc.2017.43

[4] LUTHER C, SWAMI U, ZHANG J, MILHEM M, ZAKHARIA Y. Advanced stage melanoma therapies: detailing the present and exploring the future. Crit Rev Oncol Hematol 2019; 133: 99–111. https://doi.org/10.1016/j.critrevonc.2018.11.002

[5] YU P, HUANG B, SHEN M, LAU C, CHAN E et al. p15(PAF), a novel PCNA associated factor with increased expression in tumor tissues. Oncogene 2001; 20: 484–489. https://doi.org/10.1038/sj.onc.1204113

[6] DE MARCH M, BARRERA-VILARMAU S, CRESPAN E, MENTEGARI E, MERINO N et al. p15PAF binding to PCNA modulates the DNA sliding surface. Nucleic Acids Res 2018; 46: 9816–9828. https://doi.org/10.1093/nar/gky723

[7] SLADE D. Maneuvers on PCNA rings during DNA replication and repair. Genes (Basel) 2018; 9: 416. https://doi.org/10.3390/genes9080416

[8] SIMPSON F, LAMMERTS VAN BUEREN K, BUTTERFIELD N, BENNETTS JS, BOWLES J et al. The PCNA-associated factor KIAA0101/p15(PAF) binds the potential tumor suppressor product p33ING1b. Exp Cell Res 2006; 312: 73–85. https://doi.org/10.1016/j.yexcr.2005.09.020

[9] JUN S, LEE S, KIM HC, NG C, SCHNEIDER AM et al. PAF-mediated MAPK signaling hyperactivation via LAMTOR3 induces pancreatic tumorigenesis. Cell Rep 2013; 5: 314–322. https://doi.org/10.1016/j.celrep.2013.09.026

[10] LV W, SU B, LI Y, GENG C, CHEN N. KIAA0101 inhibition suppresses cell proliferation and cell cycle progression by promoting the interaction between p53 and Sp1 in breast cancer. Biochem Biophys Res Commun 2018; 503: 600–606. https://doi.org/10.1016/j.bbrc.2018.06.046

[11] LIU X, CHENG C, CAI Y, GU Y, WU Y et al. Pan-cancer analyses reveal the regulation and clinical outcome association of PCLAF in human tumors. Int J Oncol 2022; 60: 66. https://doi.org/10.3892/ijo.2022.5356

[12] TANG Z, KANG B, LI C, CHEN T, ZHANG Z. GEPIA2: an enhanced web server for large-scale expression profiling and interactive analysis. Nucleic Acids Res 2019; 47: W556–W560. https://doi.org/10.1093/nar/gkz430

[13] HOADLEY KA, YAU C, HINOUE T, WOLF DM, LAZAR AJ et al. Cell-of-origin patterns dominate the molecular classification of 10,000 tumors from 33 types of cancer. Cell 2018; 173: 291–304.e6. https://doi.org/10.1016/j.cell.2018.03.022

[14] LEE E, CHUANG HY, KIM JW, IDEKER T, LEE D. Inferring pathway activity toward precise disease classification. PLoS Comput Biol 2008; 4: e1000217. https://doi.org/10.1371/journal.pcbi.1000217

[15] LIAO C, WANG X. TCGAplot: an R package for integrative pan-cancer analysis and visualization of TCGA multiomics data. BMC Bioinformatics 2023; 24: 483. https://doi.org/10.1186/s12859-023-05615-3

[16] WANG B, WANG M, ZHANG W, XIAO T, CHEN CH et al. Integrative analysis of pooled CRISPR genetic screens using MAGeCKFlute. Nat Protoc 2019; 14: 756–780. https://doi.org/10.1038/s41596-018-0113-7

[17] SUBRAMANIAN A, TAMAYO P, MOOTHA VK, MUKHERJEE S, EBERT BL et al. Gene set enrichment analysis: a knowledge-based approach for interpreting genome-wide expression profiles. Proc Natl Acad Sci U S A 2005; 102: 15545–15550. https://doi.org/10.1073/pnas.0506580102

[18] YUAN H, YAN M, ZHANG G, LIU W, DENG C et al. CancerSEA: a cancer single-cell state atlas. Nucleic Acids Res 2019; 47: D900–D908. https://doi.org/10.1093/nar/gky939

[19] HÄNZELMANN S, CASTELO R, GUINNEY J. GSVA: gene set variation analysis for microarray and RNA-seq data. BMC Bioinformatics 2013; 14: 7. https://doi.org/10.1186/1471-2105-14-7

[20] MATTHEWS HK, BERTOLI C, DE BRUIN RAM. Cell cycle control in cancer. Nat Rev Mol Cell Biol 2022; 23: 74–88. https://doi.org/10.1038/s41580-021-00404-3

[21] XIE C, YAO M, DONG Q. Proliferating cell unclear antigen-associated factor (PAF15): a novel oncogene. Int J Biochem Cell Biol 2014; 50: 127–131. https://doi.org/10.1016/j.biocel.2014.02.024

[22] KIM MJ, CERVANTES C, JUNG YS, ZHANG X, ZHANG J et al. PAF remodels the DREAM complex to bypass cell quiescence and promote lung tumorigenesis. Mol Cell 2021; 81: 1698–1714. https://doi.org/10.1016/j.molcel.2021.02.001

[23] LIU X, CAI Y, CHENG C, GU Y, HU X et al. PCLAF promotes neuroblastoma G1/S cell cycle progression via the E2F1/PTTG1 axis. Cell Death Dis 2022; 13: 178. https://doi.org/10.1038/s41419-022-04635-w

[24] HOSOKAWA M, TAKEHARA A, MATSUDA K, EGUCHI H, OHIGASHI H et al. Oncogenic role of KIAA0101 interacting with proliferating cell nuclear antigen in pancreatic cancer. Cancer Res 2007; 67: 2568–2576. https://doi.org/10.1158/0008-5472.CAN-06-4356

[25] WANG X, JUNG YS, JUN S, LEE S, WANG W et al. PAF-Wnt signaling-induced cell plasticity is required for maintenance of breast cancer cell stemness. Nat Commun 2016; 7: 10633. https://doi.org/10.1038/ncomms10633

[26] GUO M, LI J, WAN D, GU J. KIAA0101 (OEACT-1), an expressionally down-regulated and growth-inhibitory gene in human hepatocellular carcinoma. BMC Cancer 2006; 6: 109. https://doi.org/10.1186/1471-2407-6-109

[27] TANTIWETRUEANGDET A, PANVICHIAN R, SORNMAYURA P, LEELAUDOMLIPI S, MACOSKA JA. PCNA-associated factor (KIAA0101/PCLAF) overexpression and gene copy number alterations in hepatocellular carcinoma tissues. BMC Cancer 2021; 21: 295. https://doi.org/10.1186/s12885-021-07994-3

[28] HOU M, ZHAO Z, LI S, ZHANG Z, LI X et al. Single-cell analysis unveils cell subtypes of acral melanoma cells at the early and late differentiation stages. J Cancer 2025; 16: 898–916. https://doi.org/10.7150/jca.102045

[29] LIU L, CHEN X, XIE S, ZHANG C, QIU Z et al. Variant 1 of KIAA0101, overexpressed in hepatocellular carcinoma, prevents doxorubicin-induced apoptosis by inhibiting p53 activation. Hepatology 2012; 56: 1760–1769. https://doi.org/10.1002/hep.25834

[30] WANG H, GUO M, WEI H, CHEN Y. Targeting p53 pathways: mechanisms, structures, and advances in therapy. Signal Transduct Target Ther 2023; 8: 92. https://doi.org/10.1038/s41392-023-01347-1

[31] YU Y, XIAO X, JIN F. Inhibition of KIAA0101 expression can regulate cell proliferation and apoptosis in colon cancer. Cancer Biother Radiopharm 2025; 40: 662–671. https://doi.org/10.1089/cbr.2025.0108

[32] JIN C, LIU Z, LI Y, BU H, WANG Y et al. PCNA-associated factor P15(PAF), targeted by FOXM1, predicts poor prognosis in high-grade serous ovarian cancer patients. Int J Cancer 2018; 143: 2973–2984. https://doi.org/10.1002/ijc.31800

[33] JIA YS, YANG L, ZHU YQ, MA CB. Beta-catenin knockdown impairs the viability of ovarian cancer cells by modulating YAP-dependent glycolysis. Am J Transl Res 2023; 15: 982–994.

[34] LI Y, ZENG ZW, CHEN D, GU ZC, YAN WL et al. Facilitated drug repurposing with Artemisinin-derived PROTACs: unveiling PCLAF as a therapeutic target. J Med Chem 2023; 66: 11335–11350. https://doi.org/10.1021/acs.jmedchem.3c00824

[35] KIM MJ, XIA B, SUH HN, LEE SH, JUN S et al. PAF-Myc-controlled cell stemness is required for intestinal regeneration and tumorigenesis. Dev Cell 2018; 44: 582–596.e4. https://doi.org/10.1016/j.devcel.2018.02.010

[36] CHENG Y, LI K, DIAO D, ZHU K, SHI L et al. Expression of KIAA0101 protein is associated with poor survival of esophageal cancer patients and resistance to cisplatin treatment in vitro. Lab Invest 2013; 93: 1276–1287. https://doi.org/10.1038/labinvest.2013.124

[37] ZHU K, DIAO D, DANG C, SHI L, WANG J et al. Elevated KIAA0101 expression is a marker of recurrence in human gastric cancer. Cancer Sci 2013; 104: 353–359. https://doi.org/10.1111/cas.12083

[38] CHEN Y, JIN Y, YING H, ZHANG P, CHEN M et al. Synergistic effect of PAF inhibition and X-ray irradiation in non-small cell lung cancer cells. Strahlenther Onkol 2021; 197: 343–352. https://doi.org/10.1007/s00066-020-01708-7

https://doi.org/10.4149/neo_2025_250720N317

PAF15 drives melanoma progression by promoting proliferation concomitant with suppression of DNA damage and apoptosis: a novel therapeutic vulnerability

Yacong JI[1,#], Chongyang LI[2,#], Han HAO[3], Yang LIU[4], Yan MAO[1], Leiyang GUO[1], Lichao LIU[1], Yaling LIU[1], Shaomin SHI[1,*]

Supplementary Information

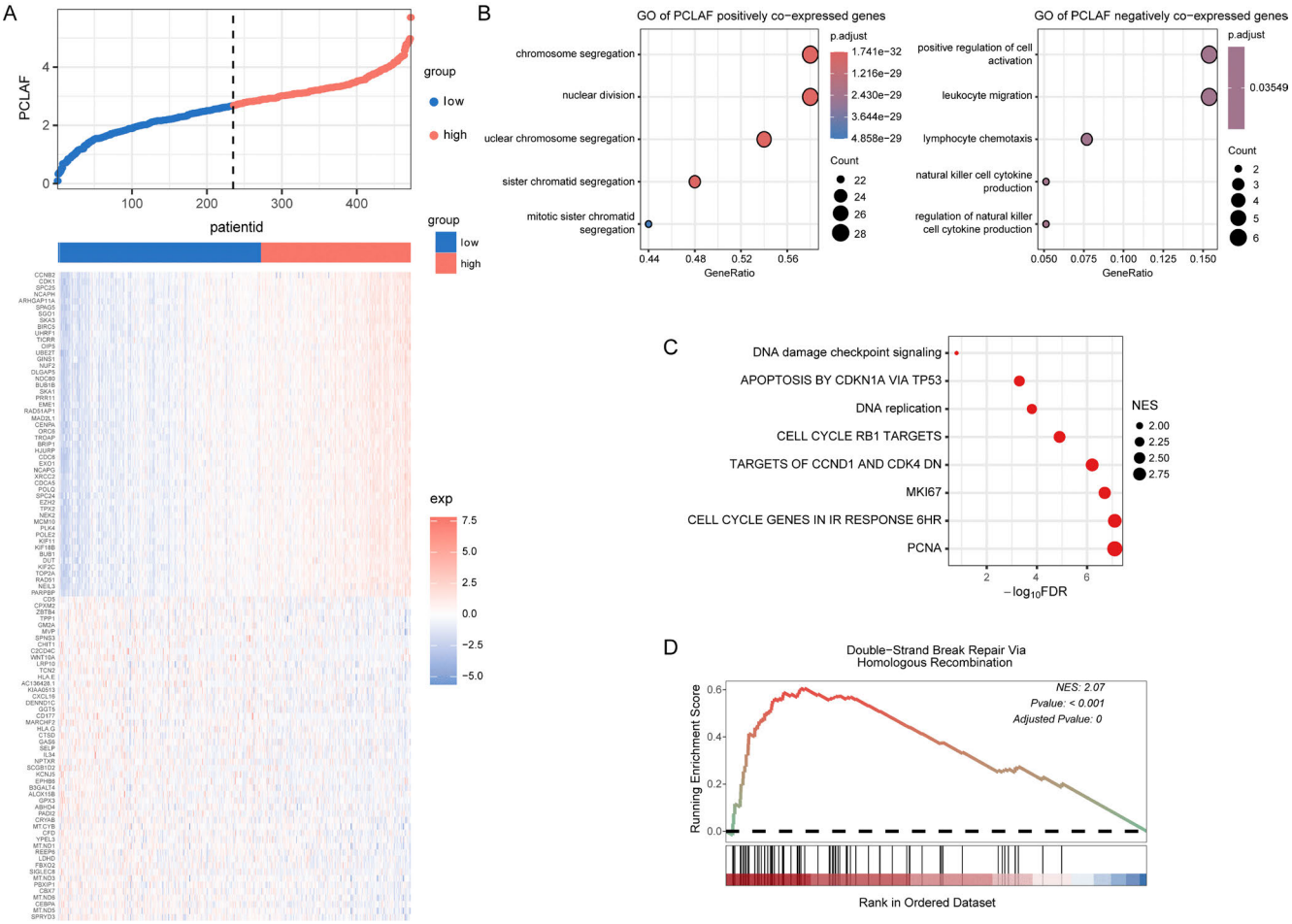

Supplementary Figure S1. Enrichment analysis of TCGA-SKCM data. A) The expression levels of PAF15 in different SKCM patients in TCGA. Heatmap depicting the differential expression of genes related to biological regulation in SKCM patients with high and low expression of the PAF15 gene. B) Bubble plots depicting GO enrichment analysis of co-expressed genes positively and negatively correlated with PAF15. C) GSEA of PAF15-high vs PAF15-low TCGA-SKCM transcriptomic data. D) Ridge plot of the enriched pathway "Double-Strand Break Repair Via Homologous Recombination".